Molecular Vision 2026; 32:84-100 <http://www.molvis.org/molvis/v32/84>
Received 16 May 2025 | Accepted 16 February 2026 | Published 17 February 2026

Nanobacterial detection in aqueous humor and its effect on postphacoemulsification visual acuity among highly myopic patients

Xiaoli Wu,[1] Yan Zhou,[2] Fen Lan,[3] Tao Li,[1] Juan Tang,[4] Guifang Wu,[5] Xingde Liu[1]

(The first two authors contributed equally to this work)

[1]Department of Ophthalmology, The Ziyang Central Hospital, Ziyang, China; [2]Department of Nephrology, The Ziyang Central Hospital, Ziyang, China; [3]Department of Ophthalmology, Western Theater Command General Hospital, Chengdu, China; [4]Department of Endocrinology, The Ziyang Central Hospital, Ziyang, China; [5]Center of Disinfection Supply, The Ziyang Central Hospital, Ziyang, China

This study aimed to investigate factors affecting visual outcomes after phacoemulsification in highly myopic patients with cataracts, based on the detection of nanobacteria (NB) in aqueous humor. Fifty highly myopic patients with cataracts who underwent phacoemulsification surgery at The First People's Hospital of Ziyang from December 2022 to June 2023 were enrolled. Aqueous humor samples were gathered from patients before surgery, and NB were isolated and cultured from the aqueous humor. They were identified using scanning electron microscopy and transmission electron microscopy. The calcium-phosphorus ratios in NB cultures (NB group) and nanohydroxyapatite (nHA) cultures (nHA group) were determined by energy-dispersive X-ray spectroscopy. Cell inhibition was compared using a CCK-8 assay. The expressions of calcification-related proteins, bone morphogenetic protein 2, osteopontin, apoptosis-related proteins, B-cell lymphoma 2 (Bcl-2), and Bcl-2–associated X protein in cells were examined by western blot. Based on the best-corrected visual acuity (VA) 3 months after surgery, patients were classified into a normal vision (NV) group (best-corrected VA ≥0.3) and an abnormal vision (AV) group (best-corrected VA <0.3). The factors influencing postoperative VA and efficacy were analyzed. Results revealed that the characteristics of the aqueous humor cultures were consistent with the features of NB described in the literature, with NB measuring approximately 90 to 340 nm in transmission electron microscopy. Energy-dispersive X-ray results indicated no remarkable difference in calcium-phosphorus ratios between the NB and nHA groups ($p > 0.05$), but the NB group exhibited remarkably stronger cell inhibition relative to the nHA group ($p < 0.05$). Western blot results revealed obviously higher levels of bone morphogenetic protein 2, osteopontin, and Bcl-2–associated X proteins in the NB group compared to the nHA group ($p < 0.05$), while Bcl-2 expression was sharply lower, with a great difference in the NB group ($p > 0.05$). The gap in best-corrected VA 1 month after surgery between the NV group (68%) and the AV group (32%) was obvious ($p < 0.05$). With increasing recovery time, the number of patients with best-corrected VA ≥0.3 at 6 months postoperatively substantially increased (86%). The NB-positive rate in the aqueous humor samples was observably lower in the NV group than the rate in the AV group ($p < 0.05$). Univariate logistic regression analysis revealed great differences in age, duration of high myopia, axial length (AXL), corneal astigmatism, incidence of macular disease, and NB-positive rate ($p < 0.05$). Multivariate logistic regression analysis indicated that AXL and the presence of NB in the aqueous humor were independent factors influencing the postoperative visual prognosis of highly myopic patients with cataracts ($p < 0.05$). The experimental results signified that NB cultures suppressed cells and, at the cellular level, influenced the visual recovery after surgery by regulating the expression of calcification-related proteins and mitochondrial apoptosis-related proteins. Multivariate logistic regression analysis further confirmed that AXL and the presence of NB in the aqueous humor were independent factors affecting the postoperative visual prognosis. This finding offered strong support for the future development of relevant treatment modalities.

Cataract is a condition where the eye's crystalline lens becomes opaque, leading to a decrease in the visual acuity (VA) of patients. Some studies suggest that cataracts are often associated with lens calcification and tissue hardening. The efficacy of phacoemulsification surgery becomes a matter of significant concern when cataracts are combined with high myopia. Patients with high myopia typically exhibit elongated axial length (AXL), thinner retinas, and altered ocular biomechanical properties, which increase the risk of intraoperative complications (e.g., posterior capsule rupture) and affect postoperative visual outcomes (including slower visual recovery

Correspondence to: Xingde Liu, The First People's Hospital of Ziyang, Department of Ophthalmology, The First People's Hospital of Ziyang, Ziyang, Sichuan 641300, China; FAX: 18096388268; email: Liuxingde@mjcedu.cn

and a higher incidence of retinal detachment) [1,2]. Therefore, identifying factors influencing postoperative vision recovery in this specific population is critical. Currently, the detection of nanobacteria (NB) in aqueous humor has emerged as a novel technique in ophthalmic research. Although NB has been extensively studied in conditions such as renal calculi and atherosclerosis, its presence and role in the aqueous humor of patients with cataracts, particularly those with high myopia, remain largely unexplored, representing a significant knowledge gap in the field. Detecting the presence of NB may provide deeper insights into alterations in the intraocular microenvironment, thereby offering a more precise basis for clinical management.

NB is a kind of prokaryotic microorganism, which is characterized by its extremely small size, with a diameter ranging from 20 to 200 nm. However, there is a controversy about the nature of NB. The current consensus tends to regard these particles as probably not being truly living organisms but rather abiotic mineralized nanoparticles, fragments of biofilms, and so on. In recent years, the potential role of microbial factors such as NB in aqueous humor has garnered increasing attention. Nanoparticle-based carriers have shown promise in optimizing the biocompatibility of intraocular lenses [3]; however, their detection efficacy in aqueous humor and their impact on surgical outcomes require further systematic investigation. NB exhibits typical microbial features, including a cell membrane, DNA, and other characteristic microbial traits. What sets it apart is its tiny size, unique structure, and the ability to initiate biological mineralization processes, leading to the precipitation of mineral substances [4]. Clinical studies on NB have shown a significant correlation between NB and various diseases such as kidney stones, Alzheimer's disease, atherosclerosis, gallstones, and more. It is proposed that NB is related to the process of biomineralization and may exert an effect in the generation of stones and mineral deposits [5–7]. Studies reported that NB can be cultured from bile and/or gallstones [8]. Additionally, NB exhibits certain cytotoxicity [9]. There is still a debate about whether NB is a bacterium or part of a biologic entity. However, most scholars agree that NB can slowly generate hydroxyapatite encapsulation under conditions of pH 7.4 and physiologic calcium and phosphorus concentrations. This process leads to calcification of the tissue where NB is located [10].

Cellular calcification refers to the phenomenon of calcium salt deposition within or around cells. This is a biomineralization process that typically involves the precipitation of calcium-phosphate compounds, with hydroxyapatite being the most common [11]. The detection of cellular calcification is often quantified by measuring the levels of calcification-related proteins (CRPs), such as bone morphogenetic protein 2 (BMP-2) and osteopontin (OPN). BMP-2 can induce the differentiation of stem cells into osteoblasts, promoting bone formation through the formation of hydroxyapatite. OPN is a highly expressed phosphoprotein in bone and tooth tissues with various biologic functions, including the regulation of cell adhesion, migration, differentiation, and mineralization. It is involved in the deposition of calcium-phosphate and the crystallization of hydroxyapatite [12]. Partial chondrocalcinosis often occurs in tumor treatment, and studies have suggested that hydroxyapatite not only induces calcification of cartilage but also promotes cell apoptosis simultaneously [13]. Cell apoptosis is a programmed cell death process regulated by various protein families. Hydroxyapatite is believed to potentially influence the activity of apoptosis-related proteins (ARPs), such as B-cell lymphoma 2 (Bcl-2) and Bcl-2–associated X protein (Bax), disrupt mitochondrial membrane integrity, and participate in the regulation of cell apoptosis [14].

This study aimed to investigate the impact of NB detected in aqueous humor on postoperative VA outcomes after phacoemulsification in patients with cataracts with high myopia. The primary outcome measures included best-corrected VA; visual recovery rate at 1, 3, and 6 months postoperatively; and the correlation between NB positivity and these outcomes. This work delved into the potential mechanisms of action of NB in phacoemulsification surgery for highly myopic patients with cataracts through the detection of NB in the aqueous humor. The aim is to offer a scientific foundation for the development of relevant treatment modalities.

METHODS

Experimental instruments and materials: The required materials for the experiment included the isolation and identification of NB conducted in this study. Other materials used encompassed nanohydroxyapatite (nHA) powder (H106378–100 g; Shanghai Aladdin Biochemical Technology Co., Ltd., Shanghai, China); C2BBe1 human colon cancer cells (bio-69363; American Type Culture Collection, Manassas, VA); gamma-irradiated fetal bovine serum (FBS; Thermo Fisher, Waltham, MA); 1640 culture medium (Gibco, Grand Island, NY); phosphate-buffered saline buffer (Merck, Rahway, NJ); CCK-8 assay kit (Abcam, Cambridge, UK); BMP-2 rabbit anti-human polyclonal antibody, OPN rabbit antihuman monoclonal antibody, Bcl-2 rabbit antihuman monoclonal antibody, and Bax rabbit antihuman monoclonal antibody (Wuhan Huamei Biotechnology Co., Ltd., Wuhan, China); internal control β-actin rabbit antihuman monoclonal

antibody (Abcam); skimmed milk powder (Guangzhou Jiheng Pharmaceutical Technology Co., Ltd., Guangzhou**,** China); Tween-20 (Shanghai Aladdin Biochemical Technology Co., Ltd., Shanghai, China); ECL chemiluminescence kit (Shanghai Maclin Biochemical Technology Co., Ltd.); BCA protein concentration determination kit (Sigma-Aldrich, St. Louis, MO); TBS buffer (Gibco); Coomassie brilliant blue (Wuhan Canos Technology Co., Ltd., Wuhan, China); eosin (Suzhou Alpha Bioinstrumentation Co., Ltd., Suzhou, China); deionized water (Shanghai Aladdin Biochemical Technology Co., Ltd.); RIPA lysis buffer and bovine serum albumin (BSA; Shanghai Beyotime Biotechnology Co., Ltd., Shanghai, China); Tris-buffered saline with Tween-20 (TBST) buffer (Abcam); and sodium dodecyl sulfate–polyacrylamide gel electrophoresis (SDS-PAGE; Thermo Fisher).

The required instruments for the experiment included the Hitachi H-80B low-temperature ultracentrifuge (Hitachi, Tokyo, Japan), the HH-US-A constant temperature water bath (Shanghai Hetian Scientific Instrument Co., Ltd., Shanghai, China), 0.22-μm/0.45-μm bacterial filters (Millipore, Burlington, MA), MODEL3164 CO_2 incubator (Forma Scientific, Waltham, MA), KYKY2800 SEM (Beijing Zhongke KeYi Technology Development Co., Ltd., Beijing, China), Hitachi H-7650 TEM (Hitachi), Spectra Max Plus384 fully automatic enzyme marker (Molecular Devices, San Jose, CA), 3612ES10 polyvinylidene fluoride imprint membrane (Yisheng Biotechnology Co., Ltd., Yisheng, China), VANTAGE DSI energy-dispersive X-ray spectrometer (NORAN, Blaine, MN), and DEN-1 and DEN-1B turbidity meter (Guangzhou Diancheng Biotechnology Co., Ltd., Guangzhou, China).

Culture and identification of NB:

NB culture—Patient preoperative aqueous humor samples (0.5 ml each) were collected and centrifuged in a centrifuge at 251.8 ×g for 10 min. The resulting supernatant was then sequentially filtered through 0.45-μm and 0.22-μm bacterial filters. The filtered sample was introduced to 1 ml 1640 culture medium containing gamma-irradiated FBS for cultivation (37 °C, 5% CO_2). The medium was updated every 40 days, and observations were made after the white precipitate indicated that NB had successfully been cultivated. A negative control was established by incubating an equivalent volume of complete culture medium (1640 medium containing γ-irradiated FBS) without patient aqueous humor under identical conditions (37 °C, 5% CO_2) for over 40 days, with regular observation for the formation of white precipitate. No precipitate formation was observed in any negative control, ruling out contamination from the medium or serum.

NB positivity was defined as follows: after 40 days of culture, aqueous humor samples exhibiting white precipitate visible to the naked eye were further confirmed by scanning electron microscopy (SEM) or transmission electron microscopy (TEM) to exhibit morphological characteristics consistent with NB. The NB positivity rate (%) was calculated as (number of NB-positive samples / total number of samples) × 100%.

NB identification—Morphological observations of successfully cultured NB were performed using SEM and TEM. A small amount of the white precipitate obtained after successful culture was mixed with phosphate-buffered saline buffer, followed by a 20-min centrifugation at 251.8 ×g to eliminate supernatant, and the acquired precipitate was then blended with 1640 culture medium containing 10% FBS to create a suspension. The NB suspension was dropped onto a slide, fixed with 4% glutaraldehyde, dehydrated in a gradient ethanol series, dried, and observed for morphology under a scanning electron microscope. For TEM, the NB suspension was dropped onto a copper grid with a membrane, dried, and stained with a mixture of phosphotungstic acid (10 g/l) and sodium hydroxide (5 min). After drying, the sample was observed for morphology under a TEM.

Mechanism by which NB leads to cell calcification: Given that the core pathogenic mechanism of NB involves the secretion of nHA and subsequent induction of calcification, an nHA group was included as a control in this study to differentiate whether the observed cellular effects (inhibition, calcification, apoptosis) originate from the biologic activity of NB or are solely attributable to the nHA minerals they produce. The experimental C2BBe1 human colon cancer cells were sourced from the American Type Culture Collection under batch number bio-69363. Suspensions of NB and nHA with a turbidity of 2 McFarland units were prepared and set aside. The culture of cells with NB suspension was labeled as the NB group, while the culture with nHA suspension was labeled as the nHA group. "The NB suspension and nHA suspension underwent energy-dispersive X-ray spectroscopy (EDX) analysis using an EDX analyzer with a working voltage of 200 kV.

Analysis of inhibitory cell activity: The activity inhibition levels of NB and nHA on C2BBe1 cells were assessed using the CCK-8 method. C2BBe1 cells were cultured until the logarithmic growth phase, and the cell density was set to 1×10^4/ml. A 100-μl cell suspension was seeded in a 96-well plate and incubated overnight for 24 h. NB and nHA suspensions were separately added for cultivation, and CCK-8 reagent was added on days 1, 2, and 3. After a 6-h incubation, the optical

density at 450 nm was measured using an enzyme-linked immunosorbent assay reader.

Impacts on CRPs BMP-2 and OPN: C2BBe1 cells were adjusted to 2 × 10^4/ml, and a 100-µl cell suspension was seeded in a 96-well plate for overnight incubation. After 24 h, the cells were divided into three groups: the control group (no additional treatment), the NB group, and the nHA group. Respective suspensions were then added to the NB and nHA groups. Following an additional 72 h of cultivation, cells were harvested for total protein extraction using RIPA. The concentration of extracted protein was determined using the BCA. Ten percent SDS-PAGE was used to separate total proteins. Coomassie brilliant blue was used for staining. After transfer, membrane blocking was performed with 5% BSA for 1 h, followed by staining with Ponceau S. After deionized water destaining, membrane incubation was performed overnight at 4 °C with diluted primary antibodies, including BMP-2 rabbit antihuman polyclonal antibody and OPN rabbit antihuman monoclonal antibody (dilution ratio 1:1,000). Following membrane washing with TBST, alkaline phosphatase–conjugated secondary antibodies (dilution ratio 1:5,000) were introduced, and 1-h membrane incubation was followed on a shaker. Following TBST membrane washing, chemiluminescence detection was performed according to the instructions of the ECL chemiluminescence assay kit. A gel imaging system was used for protein band visualization, with β-actin as an internal reference. ImageJ (National Institutes of Health, Bethesda, MD) was used for statistical analysis of the relative grayscale values of protein bands.

Impacts on Bcl-2 and Bax: C2BBe1 cells were adjusted 2 × 10^4/ml and seeded in a 96-well plate with 100 µl of cell suspension for overnight incubation. After 24 h, the cells were divided into three groups: the control group (no additional treatment), the NB group, and the nHA group. Respective suspensions were then added to the NB and nHA groups. Following an additional 72 h of cultivation, cells were harvested for extracting total protein using RIPA. After that, protein concentration was determined using the BCA assay kit. Ten percent SDS-PAGE was employed to separate total proteins and stained with Coomassie brilliant blue. After the transfer step, the membrane underwent blocking with 5% BSA for 1 h and subsequent staining with Ponceau S. Following deionized water destaining, the membrane was subjected to an overnight incubation at 4 °C with diluted primary antibodies, which included Bcl-2 rabbit antihuman monoclonal antibody and Bax rabbit antihuman monoclonal antibody (dilution ratio 1:1,000). The washed membrane was then exposed to TBST, and alkaline phosphatase–conjugated secondary antibodies (dilution ratio 1:5,000) were applied, followed by a 1-h incubation at room temperature on a shaker. Chemiluminescence detection was performed according to the ECL chemiluminescence assay kit instructions, and protein bands were visualized using a gel imaging system, with β-actin serving as an internal reference. Ultimately, ImageJ was used for statistical analysis of the relative grayscale values of protein bands.

Research design: This study employed a prospective cohort design. Initial in vitro experiments were conducted to investigate the biological characteristics of NB and their mechanisms in inducing calcification and apoptosis (Experimental instruments and materials and Mechanism by which NB leads to cell calcification sections). Subsequently, in a cohort of patients with high myopia and cataract undergoing phacoemulsification, aqueous humor samples were prospectively collected for NB culture. The association between NB positivity rates, along with other clinical factors, and postoperative visual outcomes was analyzed.

Analysis of related factors of NB for postoperative efficacy:

Research objects and their grouping—Fifty highly myopic patients with cataracts who underwent phacoemulsification surgery at The First People's Hospital of Ziyang from December 2022 to June 2023 were enrolled. Before the surgery, 0.5 ml of aqueous humor was extracted from each patient for NB cultivation and identification. Based on the best-corrected VA in the third month after the surgery, patients were categorized into a normal vision (NV) group (best-corrected VA ≥0.3) and an abnormal vision (AV) group (best-corrected VA <0.3). The 3-month postoperative time point was selected as the primary interval for grouping because it represents the conventional period by which refractive status and VA typically stabilize following uncomplicated phacoemulsification surgery. By this time, most postoperative inflammation and corneal edema have generally resolved. This allows for a more reliable assessment of the surgical outcomes themselves, minimizing the interference from transient postoperative issues. This study has received approval from the medical ethics committee of The First People's Hospital of Ziyang.

Patients enrolled had to satisfy the following conditions: (1) patients diagnosed as highly myopic with cataracts and treated with phacoemulsification surgery, (2) those with complete medical records, and (3) those with informed consent forms signed by themselves and their family members.

Patients with any of the following conditions had to be excluded: (1) patients with abnormal liver or kidney

function and (2) patients with diseases such as immune system abnormalities.

Observation parameters—(1) The best-corrected VA was measured for patients at 1, 3, and 6 months postoperatively.

(2) Analysis of factors influencing postoperative patient outcomes: in the third month postoperatively, statistical analysis was conducted on gender (male/female), age (≥60 years), duration of illness, AXL, corneal refractive power, corneal astigmatism, and the NB-positive rate in the aqueous humor culture for all patients.

(3) Key surgical parameters, such as phaco time and cumulative dissipated energy, were recorded and compared between the NV and AV groups to exclude significant confounding effects of the surgical procedure itself on the outcomes.

(4) Maculopathy refers to various macular diseases confirmed by preoperative optical coherence tomography, primarily including myopic macular schisis, macular atrophy, choroidal neovascularization, and macular retinal detachment/schisis. A technique roadmap of this research is illustrated in Figure 1.

Statistical analysis: Data processing was conducted using SPSS 26.0 (SPSS, Inc., Chicago, IL). Continuous variables were presented as mean ± standard deviation, and intergroup comparisons were performed with the *t* test. Categorical data were expressed as frequencies or percentages, and intergroup comparisons were performed using the χ^2 test. To analyze the impact of various factors on postoperative visual prognosis, univariate logistic regression was first performed for all potential influencing factors (including sex, age, duration of high myopia, AXL, corneal astigmatism, maculopathy, and aqueous humor NB positivity rate). Variables demonstrating statistical significance ($p < 0.05$) in the univariate analysis were incorporated into a multivariate logistic regression (MLR) model to identify independent factors affecting postoperative visual prognosis. $p < 0.05$ was considered statistically significant.

RESULTS

Identification of NB and the mechanism of calcification:

Morphological identification of NB—Typical white precipitate was observed in 21 cases (42%) of all cultured aqueous humor samples. The negative control group (culture medium only) remained clear and transparent throughout the entire incubation period, with no precipitate formation observed. The white precipitate from positive cultures was collected for electron microscopy examination. The morphological identification of the aqueous humor samples is displayed in Figure 2. Under TEM, nanometer particles appeared elliptical, forming NB with a size range of approximately 90 to 340 nm, exhibiting uneven density, as depicted in Figure 2A. Under SEM, spherical nanometer particles were observed, some with spike-like structures, representing noncellular structures consistent with the characteristics of NB reported in the literature. Thus, the aqueous humor culture was confirmed to be NB [15].

NB and nHA spectral analysis—Spectral analysis was conducted on NB and nHA, and the results are illustrated in Figure 3. NB was found to contain elements such as copper, magnesium, aluminum, phosphorus, calcium, chromium, manganese, and iron. Remarkable differences were visualized in the elemental composition between nHA and NB ($p > 0.05$), as depicted in Figure 3C. This indicates that NB and nHA were similar in their basic elemental composition.

Analysis of NB and nHA inhibitory cell activity: The inhibitory effects of NB and nHA on C2BBe1 cell activity are illustrated in Figure 4. Both NB and nHA demonstrated inhibitory effects on C2BBe1 cell activity, and these effects increased with prolonged exposure. After 1 day of cultivation, the activity in the NB group became lower in contrast to that in the nHA group, but no visible difference was observed ($p > 0.05$). However, after 2 days of cultivation, the activity in the NB group was sharply lower in comparison to that in the nHA group ($p < 0.05$). This work demonstrated that NB not only reduces cell activity through the generation of nHA but also has an inherent ability to decrease cell activity. Previous research has suggested a correlation between the pathogenic components of NB and NB self-replication [16].

Impacts of NB and nHA on BMP-2 and OPN: Figure 5 shows the protein band diagram. The impact of 72-h cultivation of C2BBe1 cells with NB and nHA on CRPs BMP-2 and OPN is presented in Figure 6. In Figure 6, compared to the control group, the expression levels of BMP-2 and OPN proteins were significantly elevated in the nHA group ($p < 0.05$). In contrast, the expression levels of BMP-2 and OPN in the NB group were not only significantly higher than those in the nHA group ($p < 0.05$) but also markedly greater than those in the control group ($p < 0.01$). These results indicate that nHA can induce cellular calcification, while NB triggers a more severe calcification response. BMP-2 and OPN in the NB group exhibited much higher expression than those in the nHA group ($p < 0.05$). The findings signified that NB can induce more severe calcification than nHA. BMP-2 is a protein with osteogenic properties, and its upregulated expression may be associated with more pronounced calcification [17]. NB might activate the BMP-2 signaling pathway, prompting cells to

develop toward bone formation, accelerating the occurrence of calcification. OPN is a protein involved in cell bone matrix formation, and the increased expression level may be related to more evident calcification [18,19]. NB could potentially modulate the intracellular expression of OPN, influencing the deposition of cell bone matrix, thereby exacerbating the calcification process. The synergistic effect of BMP-2 and OPN in the cell bone formation process, enhanced by NB, triggers a more robust cellular response, leading to a more significant calcification phenomenon [20,21].

Impacts of NB and nHA on Bcl-2 and Bax: Figure 7 shows the protein band diagram. The impact of 72-h cultivation of C2BBe1 cells with NB and nHA on ARPs, namely, Bcl-2 and Bax, is depicted in Figure 8. Compared to the control group, both the nHA and NB groups exhibited an increase in the expression level of the proapoptotic protein Bax ($p < 0.05$)

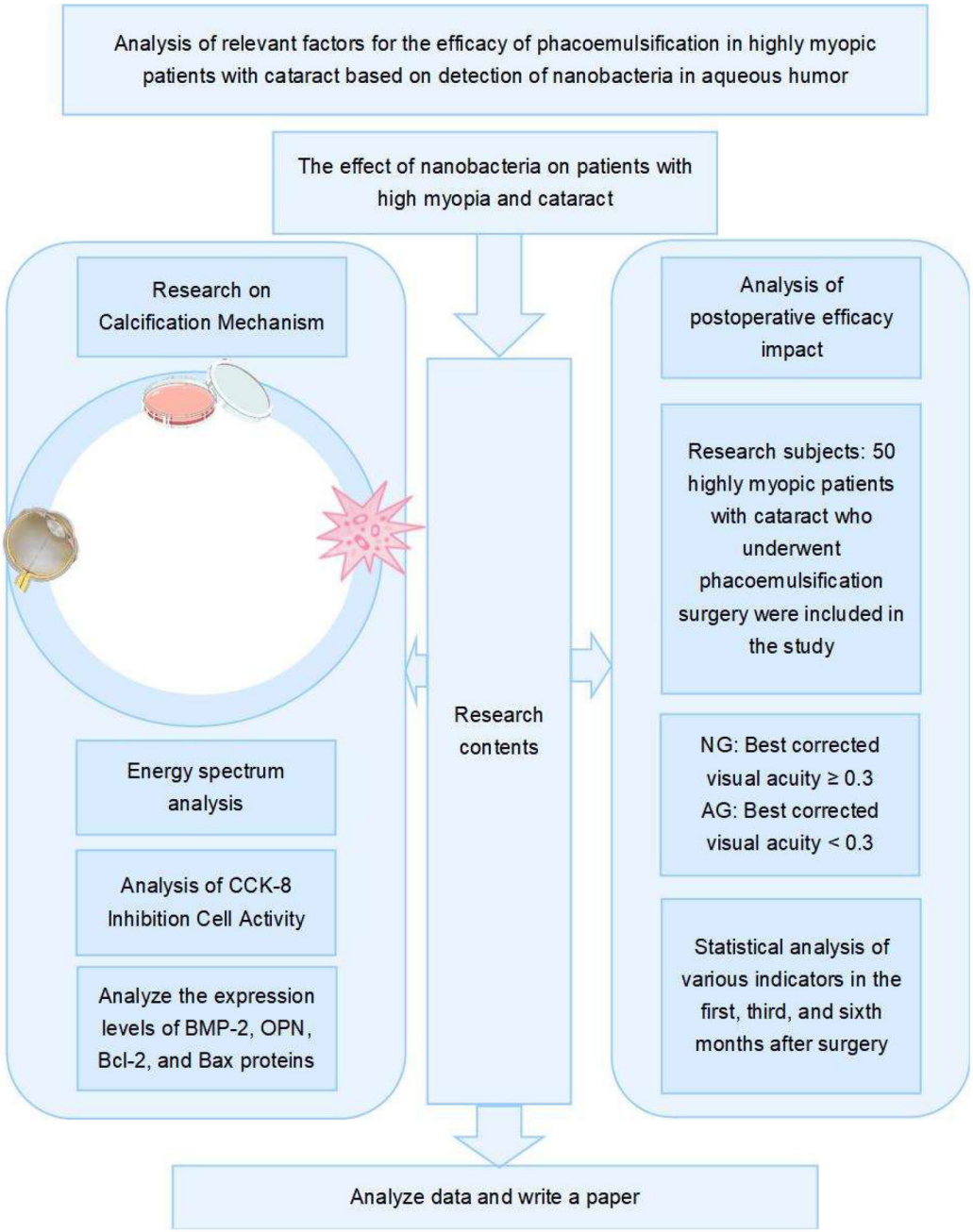

Figure 1. Flowchart of the study design.

and a decrease in the expression level of the antiapoptotic protein Bcl-2. Notably, the NB group demonstrated the most pronounced regulatory effect on the expression of these two proteins: its Bax expression was significantly higher than that in both the nHA and control groups ($p < 0.05$), while its Bcl-2 expression was significantly lower than that in both the nHA and control groups ($p < 0.05$). These results indicate that NB, compared to nHA, more effectively upregulates the proapoptotic protein Bax and downregulates the antiapoptotic protein Bcl-2, thereby more strongly activating the mitochondrial apoptosis pathway. Bax in the NB group was more strongly expressed than that in the nHA group ($p < 0.05$), while Bcl-2 demonstrated lower expression in the NB group ($p < 0.05$). This indicates that NB can regulate Bcl-2 and Bax, thereby modulating the mitochondrial pathway leading to cell apoptosis, resulting in changes in CRPs, ultimately causing cell calcification and apoptosis. Bax and Bcl-2 are key proteins in regulating the mitochondrial pathway. Upregulation of Bax and downregulation of Bcl-2 may lead to changes in mitochondrial membrane permeability, releasing apoptotic signaling molecules from the mitochondria, thereby inducing cell apoptosis [22–24]. This mechanism may be one of the reasons for the more severe calcification induced by NB. Studies have suggested that nHA, in addition to causing calcification, can induce tumor cell apoptosis when the concentration exceeds 30 μg/ml [25,26]. The higher level of calcification induced by NB may be related to its impact on cell survival status and gene expression, inducing cells to develop in a more ossified direction and increasing calcium deposition [27].

Analysis of factors related to the efficacy of NB in patients undergoing phacoemulsification surgery:

The best-corrected VA of patients—The statistical analysis of best-corrected VA for 50 patients at postoperative months 1, 3, and 6 is presented in Figure 9. As time progresses, the number of patients with best-corrected VA ≥0.3 gradually increases, reaching 82% at the sixth postoperative month. It is possible that the best-corrected VA in the first month may not have reached its optimal level, but with the passage of time, the VA of patients gradually improves. By the sixth month, 82% of patients have normal VA, indicating that the surgical outcomes stabilize over time and tend toward optimal conditions.

Patient baseline characteristics—The comparison of baseline characteristics between the two groups in this study is presented in Table 1. The results indicated that patients in the AV group were characterized by older age, longer duration of high myopia, longer AXL, higher myopic diopters, and greater corneal astigmatism. Furthermore, both the incidence of maculopathy (63.6% versus 23.1%) and the aqueous humor NB positivity rate (81.8% versus 30.8%) were significantly higher in the AV group compared to the NV group (all $p < 0.05$). No significant difference was found in gender distribution between the two groups. These findings suggest that patients with poor postoperative VA had preexisting more unfavorable ocular conditions.

Analysis of influencing factors of postoperative curative effect: Based on the best-corrected VA of patients at the third postoperative month, the patients were assigned to the NV group (39 individuals) and the AV group (11 individuals). The univariate logistic regression analysis results for factors influencing patient outcomes are presented in Figure 10. Remarkable differences were observed in terms of age, duration of high myopia, AXL, corneal astigmatism, incidence of macular disease, and NB-positive rate ($p < 0.05$). Younger patients may possess better physiologic recovery capacity, contributing to a faster postoperative VA recovery. Conversely, older patients may experience slower postoperative VA recovery due to factors such as physiologic aging.

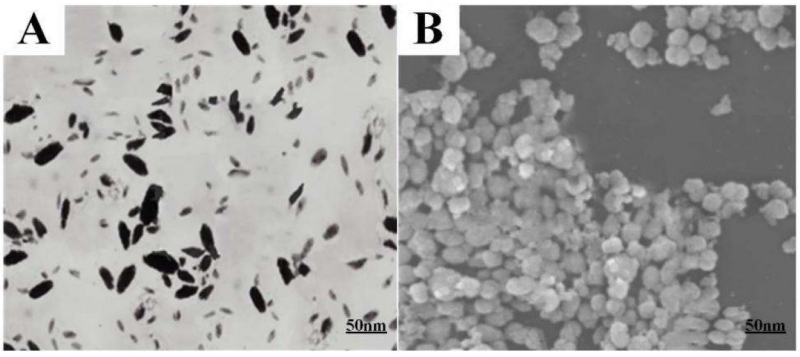

Figure 2. Morphological identification of nanobacteria under TEM and SEM.

The duration of high myopia and the resulting elongation of the eyeball significantly impact ocular structure and VA correction, thus influencing postoperative outcomes. Surgery can affect corneal shape, and greater corneal astigmatism may lead to instability in postoperative VA quality. The presence of macular disease can directly affect the macular region, influencing vision and color recognition. The existence of macular disease may increase the risk of abnormal VA after surgery, affecting the best-corrected VA of patients. The NB-positive rate in the AV group was sharply higher, in contrast to that in the NV group, indicating that NB infection can extremely impact postoperative VA recovery in patients.

Key surgical parameters were compared between the two patient groups to exclude the potential influence of procedural complexity on outcome differences. The results (Table

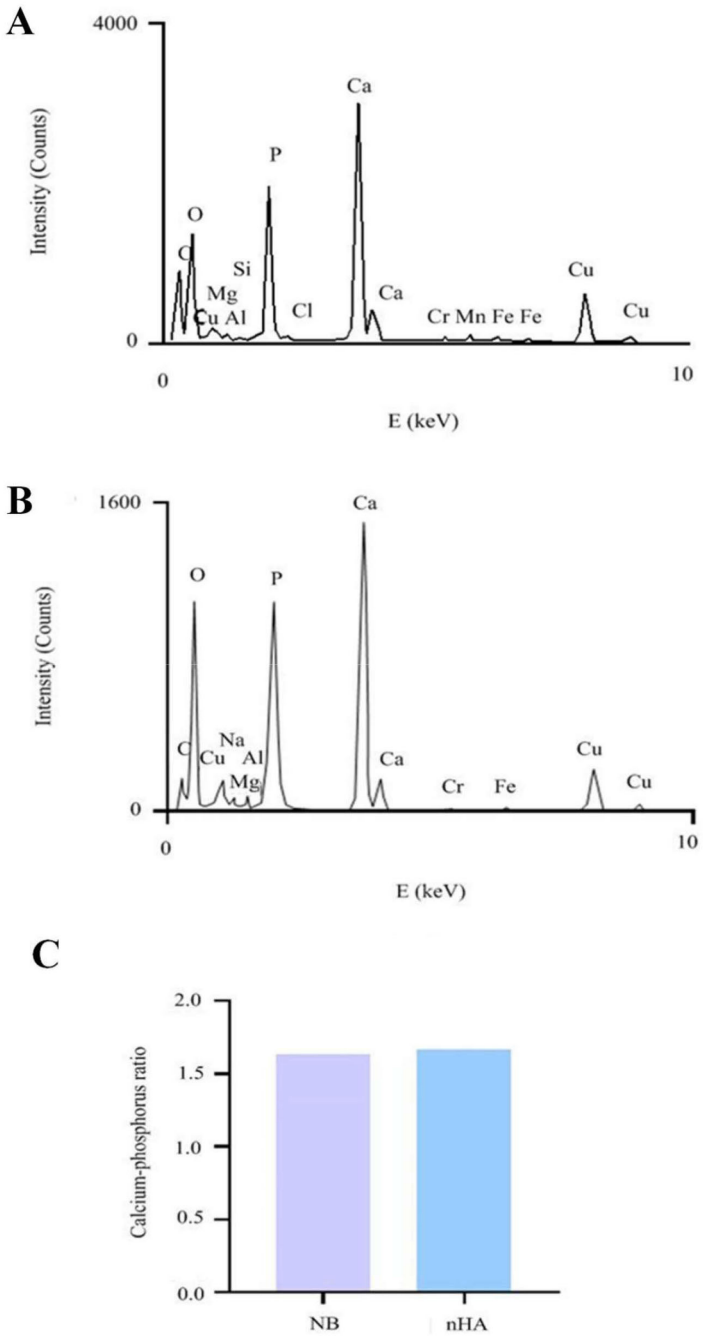

Figure 3. Energy-dispersive X-ray spectroscopy (EDX) analysis of nanobacteria and nanohydroxyapatite.

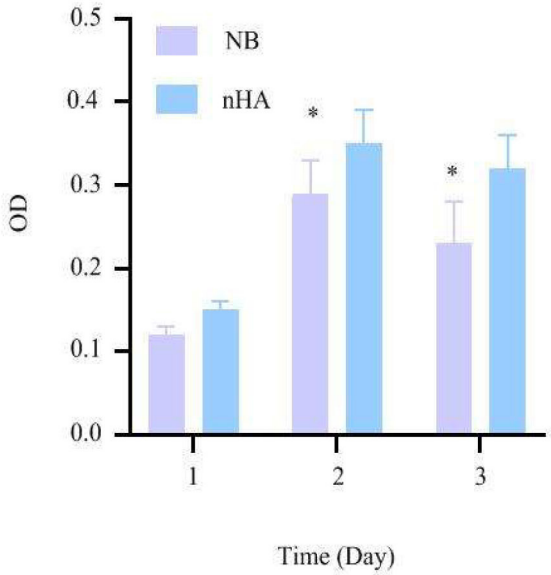

Figure 4. Inhibitory effects of nanobacteria and nanohydroxyapatite on C2BBe1 cell activity.

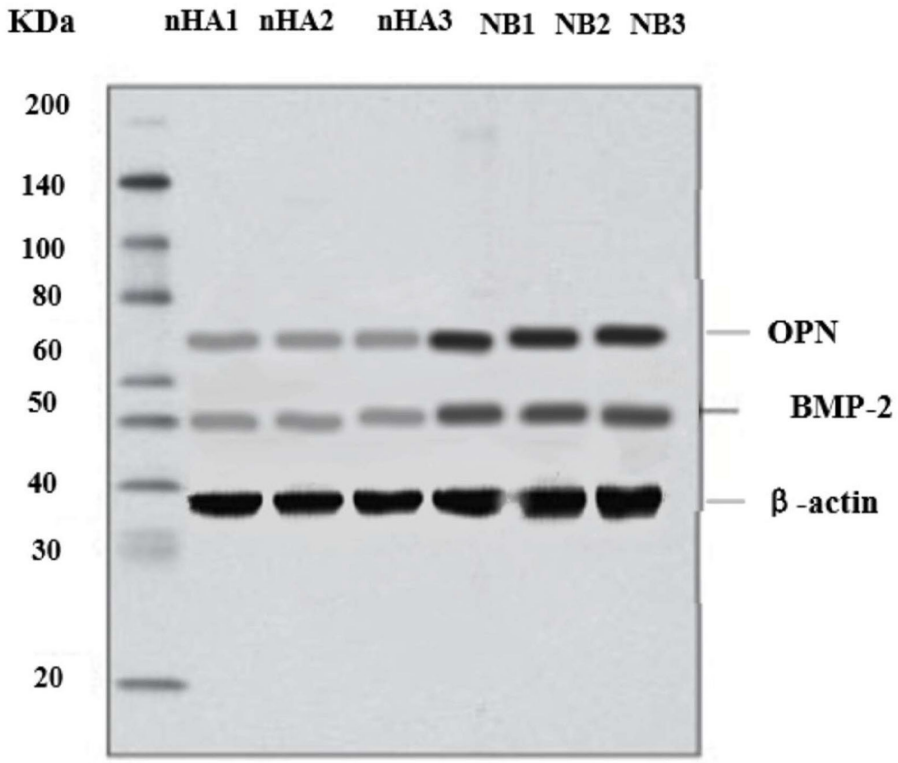

Figure 5. Protein bands of BMP-2 and OPN detected by western blot.

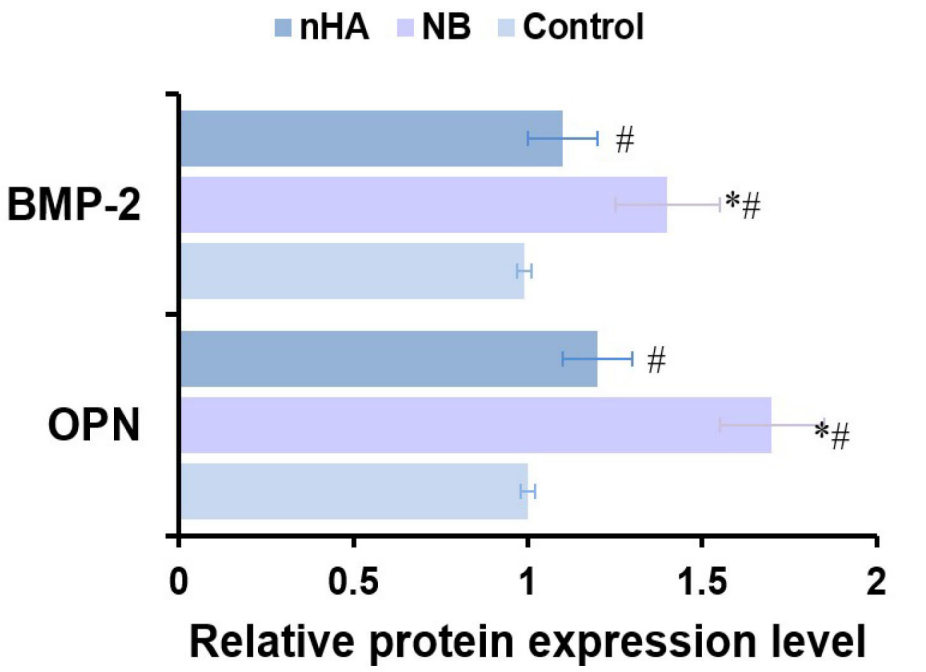

Figure 6. Expression levels of BMP-2 and OPN in C2BBe1 cells after 72-h cultivation with nanobacteria or nanohydroxyapatite.

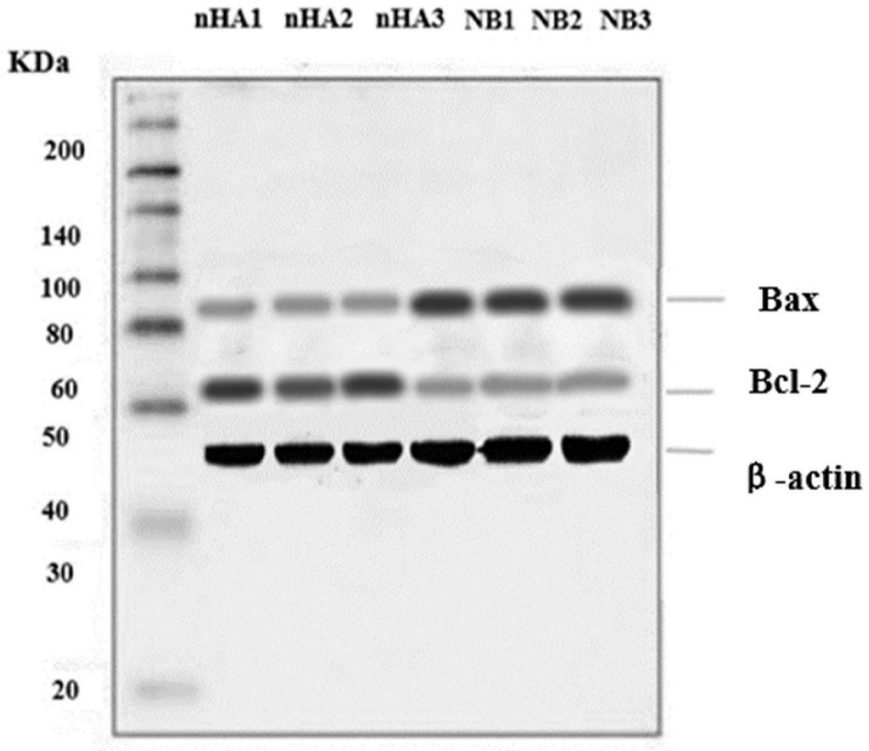

Figure 7. Protein bands of Bcl-2 and Bax detected by western blot.

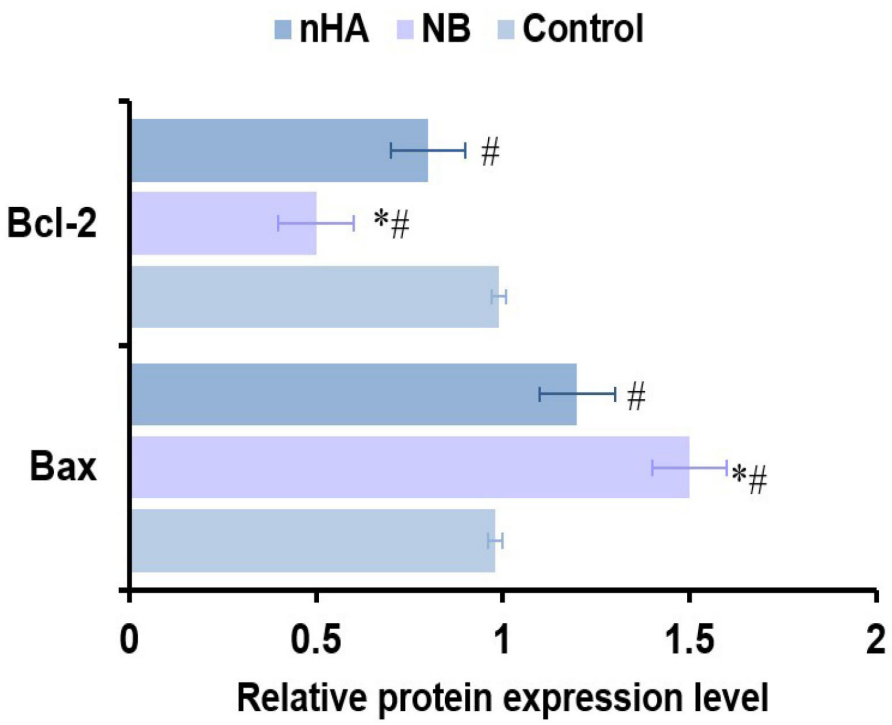

Figure 8. Expression levels of Bcl-2 and Bax in C2BBe1 cells after 72-h cultivation with nanobacteria or nanohydroxyapatite.

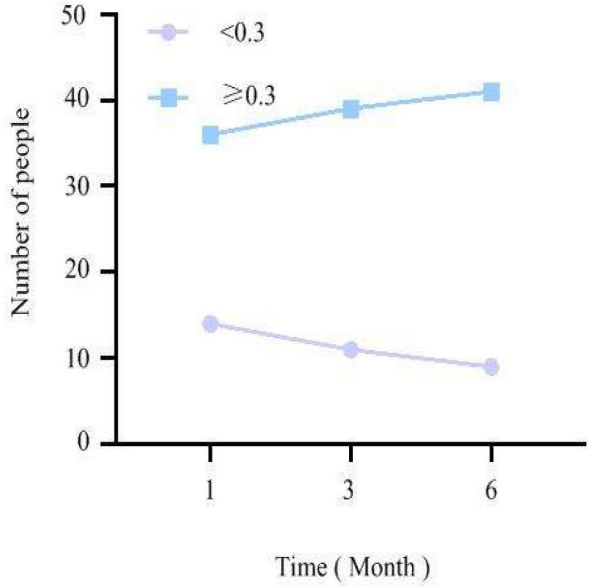

Figure 9. Best-corrected visual acuity at 1, 3, and 6 months after surgery.

Table 1. Comparison of baseline characteristics between the NV and AV groups.

Characteristics	Total (n=50)	NV group (n=39)	AV group (n=11)	*P*
Age (years)	65.2±8.5	63.1±7.9	72.4±6.8	**0.001**
Sex, Male (%)	24 (48.0)	20 (51.3)	4 (36.4)	0.376
Duration of high myopia (years)	15.6±6.2	14.2±5.5	21.3±5.1	**0.001**
Axial length (mm)	28.4±1.8	27.9±1.5	30.6±1.2	**0.001**
Spherical equivalent (D)	−12.6±3.2	−11.8±2.9	−14.9±3.5	**0.003**
Corneal astigmatism (D)	1.5±0.6	1.3±0.5	2.1±0.7	**0.001**
Concomitant maculopathy, n (%)	16 (32.0)	9 (23.1)	7 (63.6)	**0.012**
NB positivity rate, n (%)	21 (42.0)	12 (30.8)	9 (81.8)	**0.002**

Note: NV, normal vision; AV, abnormal vision; D, diopter. Bold p values indicated statistical significance (p<0.05).

2) showed no statistically significant differences between the NV and AV groups in cumulative dissipated energy (12.5% ± 3.2% versus 13.8% ± 4.1%, $p = 0.268$) or ultrasound time (45.6 ± 10.8 s versus 49.3 ± 12.4 s, $p = 0.333$). These findings indicate comparable surgical difficulty and ultrasonic energy load between the groups, suggesting that the surgical procedure itself was not the primary factor contributing to the observed differences in postoperative visual outcomes.

The factors influencing the outcomes of phacoemulsification surgery in highly myopic patients with cataracts were subjected to a multivariate logistic analysis, as presented in Table 3. AXL and NB-positive rate emerged as independent factors significantly affecting the efficacy of surgery ($p < 0.05$). This indicates that AXL and NB-positive rate have more independent and pronounced effects on the surgical outcomes.

DISCUSSION

This work delved into the identification of NB in the aqueous humor of the eye and explored its relationship with the calcification mechanism. Simultaneously, it investigated the impact of NB on the efficacy of phacoemulsification surgery in patients. The main findings encompassed the morphological characteristics of NB, results from spectral analysis, the influence on cell activity, and a comparison between NB and nHA. Additionally, through statistical analysis and examination of related factors affecting the best-corrected VA postsurgery, this work revealed the pivotal role of NB in surgical outcomes.

This work confirmed the morphological characteristics of NB in the aqueous humor of the eye, consistent with existing literature [28,29]. Furthermore, this work revealed the mechanism by which NB triggers more severe calcification by activating the BMP-2 signaling pathway and regulating OPN expression, addressing the existing gap in the literature regarding NB calcification mechanisms. Calcification is a key factor in the progression of ocular diseases and is tightly linked to the occurrence and development of ophthalmic conditions, such as retinal diseases and cataracts [30]. Abnormal calcification induced by NB could be a major contributing factor to functional impairments in the eye and reduced surgical efficacy. BMP-2 is a protein that promotes bone formation, and its pathway is crucial in skeletal development and maintenance. This work revealed that NB can activate the BMP-2 pathway, prompting cells to develop in the direction of bone formation and accelerating the occurrence of calcification. NB induces cells to release BMP-2, which may be triggered by interaction with the cell membrane or through intracellular signaling pathways. Released BMP-2 binds to receptors, forming BMP-2/receptor complexes. This activates pathways on the receptors, initiating downstream cellular responses. The BMP-2 pathway activation ultimately results in cells developing in the direction of bone formation, increasing the tendency for calcification [31]. This is a crucial step in NB-induced more severe calcification. OPN is a protein involved in cell bone matrix formation, and its expression is closely related to the calcification process. In addition, this work signified that NB, by regulating OPN expression, influences the deposition of cell bone matrix, thereby exacerbating the calcification process. NB-induced signal transduction may enhance the transcription and translation processes of the OPN gene. This results in the synthesis and release of more OPN protein into the extracellular space. The increase in OPN leads to more calcium ions binding to the cell matrix, forming more stable calcification structures [32]. This exacerbates the calcification phenomenon induced by NB.

The finding that NB induces significant calcification and apoptosis at the cellular level raises the question of how

this process specifically affects postoperative VA in patients. One potential mechanism is that NB-induced calcification may lead to a higher incidence or earlier onset of posterior capsular opacification (PCO), a common complication after cataract surgery that can cause blurred vision. The deposition of calcium phosphate complexes on the posterior capsule may serve as foci for lens epithelial cell proliferation and migration, thereby accelerating PCO formation and resulting in slower visual recovery or the need for additional interventions [33]. Beyond the lens, the presence of NB and the associated calcific microenvironment in the aqueous humor may adversely affect other delicate ocular structures. Calcification could impair trabecular meshwork function, potentially influencing intraocular pressure, or contribute to macular dysfunction by promoting local inflammation or disrupting the retinal pigment epithelium–photoreceptor complex [34].

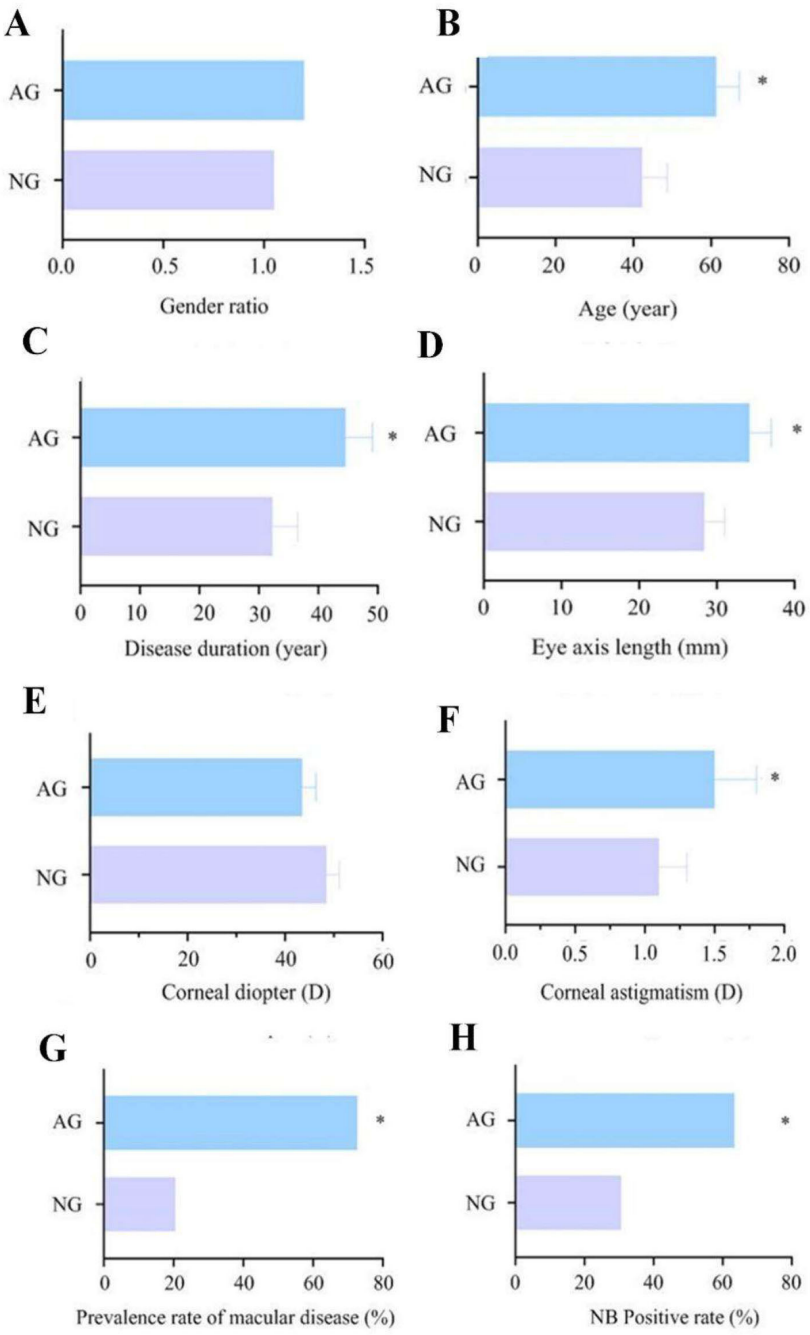

Figure 10. Univariate logistic regression analysis of factors influencing postoperative visual acuity.

Table 2. Comparison of surgical parameters between NV group and AV group patients.

Group	Case number	CDE (%)	Ultrasound time (s)
NV group	39	12.5±3.2	45.6±10.8
AV group	11	13.8±4.1	49.3±12.4
t		−1.12	−0.98
P		0.268	0.335

Although this study did not directly measure PCO incidence or macular pathology using methods such as optical coherence tomography (OCT), the significant association between NB positivity and poorer short-term visual outcomes is consistent with the hypothesis that NB-induced pathological calcification impedes optimal visual rehabilitation by affecting both anterior and posterior segment structures.

The observed upregulation of BMP-2 and OPN induced by NB, along with the shift in the Bax/Bcl-2 ratio toward a proapoptotic state, necessitates an exploration of their specific roles in ocular pathophysiology. In the eye, BMP-2 signaling is not only critical for bone formation but also implicated in the pathological calcification of intraocular tissues, such as potentially exacerbating calcification of the lens capsule or retinal pigment epithelium, which could worsen posterior capsular opacification or disrupt the outer blood–retinal barrier [35,36]. Similarly, OPN, a key regulator of biomineralization, is upregulated in various calcification-associated ocular conditions, including band keratopathy and drusen formation in age-related macular degeneration. Its overexpression likely promotes the nucleation and growth of hydroxyapatite crystals in the unique microenvironment of the aqueous or vitreous humor [37,38]. Dysregulation of the mitochondrial apoptotic pathway, evidenced by an increased Bax/Bcl-2 ratio, is a well-established mechanism in lens epithelial cell apoptosis during cataractogenesis [39]. In the retina, an imbalance toward proapoptotic signaling can trigger the death of photoreceptors and ganglion cells, a common terminal pathway in many retinal degenerative diseases [40]. Therefore, the ability of NB to concurrently drive calcification-associated protein expression and promote a proapoptotic cellular state provides a plausible dual pathogenic mechanism for its impairment of postoperative visual recovery: potentially affecting both the clarity of the optical pathway and the health of the neurosensory retina.

An interesting finding in the longitudinal follow-up of this study was that the proportion of patients with a best-corrected VA ≥0.3 increased from 68% at 1 month to 86% at 6 months. This trend suggests that a subset of patients experienced delayed visual recovery. At the 3-month time point, the NB positivity rate was significantly higher in the AV group. It is hypothesized that NB-driven pathological processes, such as chronic low-grade intraocular inflammation, persistent calcification, or delayed apoptosis, may impede the pace of postoperative visual rehabilitation. Therefore, the 3-month postoperative time point, while reflecting stable outcomes in most patients, effectively captures this delay in visual recovery associated with the presence of NB. The subsequent improvement observed at 6 months may be attributed to the gradual resolution of these NB-related effects, neuroadaptive changes, or the slower remodeling of damaged ocular tissues. Thus, using 3-month postoperative VA for grouping not only aligns with routine clinical practice but also serves as a sensitive indicator for identifying patients at risk of slow recovery, in which NB may play an adverse role.

MLR analysis revealed that longer AXL and aqueous humor NB positivity were independent risk factors for poor postoperative visual prognosis after adjusting for other confounding factors. This indicates that although univariate analysis showed associations between various factors (e.g., age, disease duration, corneal astigmatism, and maculopathy) and visual prognosis, the effects of some factors may overlap or interact with other variables. For example, the occurrence of maculopathy is closely related to axial elongation, and its impact may be represented or partially explained by AXL, a more fundamental anatomic indicator. Similarly, age and disease duration may also be intrinsically linked to

Table 3. Logistic analysis of multiple factors affecting postoperative VA prognosis.

Variable	β	SEM	Wald χ^2	P	OR
AXL	0.784	0.453	5.395	0.547	2.165 (1.352 ~1.442)
NB-positive rate	1.532	0.638	2.331	0.351	5.362(1.247 ~14.295)

AXL growth. Consequently, the significance of AXL and NB remained in the multivariate model, highlighting their core independent roles in influencing postoperative visual recovery in highly myopic patients with cataracts. This finding, for the first time, validates their independent effects on surgical outcomes within a multivariate model, overcoming limitations inherent in univariate analyses. Naturally, the success of phacoemulsification surgery is influenced by multiple factors. Beyond the patient-specific anatomic factors (AXL) and biomicroenvironmental factors (NB) examined in this study, surgical parameters (e.g., ultrasonic energy and operation time), surgeon experience, postoperative inflammatory responses, and undetected macular pathologies (e.g., occult macular schisis) may also significantly impact final visual outcomes. While this study mitigated confounding effects from basic factors like age and disease duration through multivariate analysis, it did not comprehensively record or analyze all surgical parameters, representing a limitation. Therefore, our conclusions should be interpreted as follows: after adjusting for known confounding factors, AXL and NB are significant predictors, but they are not the sole determinants of visual outcomes.

The limitations of the study primarily lie in the relatively small sample size, requiring larger-scale clinical studies to validate the universality of the conclusions. Future research could expand the sample size to further confirm the role of NB in ocular diseases. Considering the significant impact of NB on the efficacy of phacoemulsification surgery in patients, further exploration of the source and dissemination pathways of NB could lead to more effective prevention and treatment strategies. Moreover, investigating the relationship between NB and other ocular diseases could provide additional insights for comprehensive treatment approaches in ophthalmology. This could contribute to improving surgical efficacy, reducing postoperative complications, and ultimately enhancing the quality of life for patients.

CONCLUSION: In summary, this study suggests that NB cultured from aqueous humor exhibits considerable inhibitory effects on cells and influences the recovery of postoperative VA by modulating the expression of CRPs and ARPs. MLR analysis further indicated that longer AXL and aqueous humor NB positivity were significantly associated with poorer postoperative visual outcomes. However, this study has several limitations, including a limited sample size and incomplete assessment of potential confounding factors such as surgical parameters. Future studies with larger sample sizes, prospective designs, and more comprehensive perioperative indicators are needed to validate these findings and further elucidate the specific mechanisms of NB in ocular diseases.

ACKNOWLEDGMENTS

Declarations/Ethics approval and consent to participate: The experimental protocol was established, according to the ethical guidelines of the Helsinki Declaration and was approved by the Human Ethics Committee of The First People's Hospital of Ziyang. Written informed consent was obtained from individual or guardian participants.

Consent for publication: Not Applicable.

Availability of data and materials: The data sets used and/or analyzed during the current study are available from the corresponding author on reasonable request.

Competing interests: There are no conflicts to declare.

Funding: The research is supported by: This project was supported by 2024 Hebei Province Medical Science Research Project Plan (20240294); The Science and Technology Project of Sichuan Provincial Health Commission (No. 24WSXT096 and No. 24WSXT098); Research Project of Sichuan Medical and Health Promotion Association in 2024 (No. KY2024QN0082); 2024 Medical Research Projects and Youth Innovation Projects of Sichuan Medical Association (No. Q2024062); The Chengdu Medical College Institute of Drug Research (25LHYW2-01 and 25LHYW2-02).

Authors' contributions: Xiaoli Wu and Yan Zhou wrote the main manuscript text; Fei Lan and Tao Li prepared figures and tables; Juan Tang, Guifang Wu, Xingde Liu revised this paper critically. All authors reviewed the manuscript. Thank the First People's Hospital of Ziyang and Western Theater Command General Hospital for all the necessary support in this research. Dr. Xiaoli Wu (Wuxiaoli@mjcedu.cn) and Dr. Xingde Liu (Liuxingde@mjcedu.cn) are co-corresponding authors.

REFERENCES

1. Shah R, Vlasak N, Evans BJW. High myopia: Reviews of myopia control strategies and myopia complications. Ophthalmic Physiol Opt 2024; 44:1248-60. [PMID: 39082137].

2. Mehta NJ, Mehta SN. Nanotechnology in Retinal Disease: Current Concepts and Future Directions. J Ocul Pharmacol Ther 2024; 40:3-12. [PMID: 38052063].

3. Kuang G, Li Y, Li Z, Ou Y, Li Z. Phacoemulsification Plus Intraocular Lens Implantation with Gold Nanoparticles for Complicated Cataract Secondary to Uveitis: Efficacy Analysis J Biomed Nanotechnol 2024; 20:1011-7. J.

4. Fayez Hassan N, Khaled Ibrahim M, Yousef El Tablawy S, Abd Allah Farrag H. Characterization of Biofilm Producer Nanobacteria Isolated from Kidney Stones of Some Egyptian Patients. Pak J Biol Sci 2021; 24:953-70. [PMID: 34585548].

5. DiCecco LA, Tang T, Sone ED, Grandfield K. Exploring Biomineralization Processes Using In Situ Liquid Transmission Electron Microscopy: A Review. Small 2025; 21:e2407539[PMID: 39523734].

6. Jin M, He B, Cai X, Lei Z, Sun T. Research progress of nanoparticle targeting delivery systems in bacterial infections. Colloids Surf B Biointerfaces 2023; 229:113444[PMID: 37453264].

7. Xie G, Zou Y, Sheng G, Yang M. Predictive value of nanobacteria for diagnosis, efficacy, and recurrence risk in coronary heart disease patients. Nanosci Nanotechnol Lett 2020; 12:696-701. .

8. Li S, Wu J, Bin B. Mechanism of influence of calcified nanoparticles in the development of calcified diseases (Review). Biomed Rep 2025; 22:102-Review[PMID: 40322555].

9. Lu H, Niu L, Yu L, Jin K, Zhang J, Liu J, Zhu X, Wu Y, Zhang Y. Cancer phototherapy with nano-bacteria biohybrids. J Control Release 2023; 360:133-48. [PMID: 37315693].

10. Villa-Bellosta R. Vascular Calcification: A Passive Process That Requires Active Inhibition. Biology (Basel) 2024; 13:111-[PMID: 38392329].

11. Sánchez-Bayuela T, Peral-Rodrigo M, Parra-Izquierdo I, López J, Gómez C, Montero O, Pérez-Riesgo E, San Román JA, Butcher JT, Sánchez Crespo M, García-Rodríguez C. Inflammation via JAK-STAT/HIF-1α Drives Metabolic Changes in Pentose Phosphate Pathway and Glycolysis That Support Aortic Valve Cell Calcification. Arterioscler Thromb Vasc Biol 2025; 45:e232-49. [PMID: 40308196].

12. Peng Y, Peng H, Ke W. Influence mechanism of osteopontin on renal injury in patients with hereditary hypercalcemia by Enzyme-linked immunosorbent assay. Cell Mol Biol (Noisy-le-grand) 2023; 69:58-62. [PMID: 37571900].

13. Oh YW, Kang SW, Park S, Park SW, Yi HG. Collagen/Hydroxyapatite Hydrogels Promote Intercellular Interactions and Osteogenic Differentiation. J Biomed Mater Res B Appl Biomater 2025; 113:e35632[PMID: 40785256].

14. Li J, Yi X, Liu L, Wang X, Ai J. Advances in tumor nanotechnology: theragnostic implications in tumors via targeting regulated cell death. Apoptosis 2023; 28:1198-215. [PMID: 37184582].

15. Cisar JO, Xu DQ, Thompson J, Swaim W, Hu L, Kopecko DJ. An alternative interpretation of nanobacteria-induced biomineralization. Proc Natl Acad Sci U S A 2000; 97:11511-5. [PMID: 11027350].

16. Erdemir F, Karabulut A, Ozveren B, Kocagoz T. How much do we know about nanobacteria? Ecotoxicol Environ Saf 2024; 288:117415[PMID: 39615305].

17. Wang M, Xu C, Zheng Y, Pieterse H, Sun Z, Liu Y. In vivo validation of osteoinductivity and biocompatibility of BMP-2 enriched calcium phosphate cement alongside retrospective description of its clinical adverse events. Int J Implant Dent 2024; 10:47-[PMID: 39472366].

18. Schroeder ME, Batan D, Gonzalez Rodriguez A, Speckl KF, Peters DK, Kirkpatrick BE, Hach GK, Walker CJ, Grim JC, Aguado BA, Weiss RM, Anseth KS. Osteopontin activity modulates sex-specific calcification in engineered valve tissue mimics. Bioeng Transl Med 2022; 8:e10358[PMID: 36684107].

19. Edanami N, Yoshiba K, Ibn Belal RS, Yoshiba N, Takenaka S, Ohkura N, Takahara S, Ida T, Baldeon R, Kasimoto S, Thongtade P, Noiri Y. Role of Dystrophic Calcification in Reparative Dentinogenesis After Rat Molar Pulpotomy. Int J Mol Sci 2025; 26:7130-[PMID: 40806263].

20. Kuzan A, Chwiłkowska A, Maksymowicz K, Abramczyk U, Gamian A. Relationships between Osteopontin, Osteoprotegerin, and Other Extracellular Matrix Proteins in Calcifying Arteries. Biomedicines 2024; 12:847-[PMID: 38672202].

21. Sivaguru M, Schrup SE, Fouke KW, Sherman ME, Samuel AZ, Maimone S, Bhargava R, Fouke BW. Mechanisms of osteopontin-stabilized amorphous calcium phosphate calcification in benign and pre-malignant breast disease. Sci Rep 2025; 15:23849-[PMID: 40615470].

22. Wan C, Liu S, Zhao L, Chang C, Li H, Li R, Chen B. Curcumin protects rat endplate chondrocytes against IL-1β-induced apoptosis via Bcl-2/Bax regulation. J Mol Histol 2025; 56:111-[PMID: 40106034].

23. Li Y, Tang L, Dang G, Ma M, Tang X. Scinderin Promotes Hydrogen Peroxide-induced Lens Epithelial Cell Injury in Age-related Cataract. Curr Mol Med 2024; 24:1426-36. [PMID: 37936437].

24. Tian X, Wei J. Sestrin 2 protects human lens epithelial cells from oxidative stress and apoptosis induced by hydrogen peroxide by regulating the mTOR/Nrf2 pathway. Int J Immunopathol Pharmacol 2024; 38:3946320241234741[PMID: 38379215].

25. Alshemary AZ, Hussain R, Dalgic AD, Evis Z. Bactericidal and in vitro osteogenic activity of nano sized cobalt-doped silicate hydroxyapatite. Ceram Int 2022; 48:28231-9. .

26. Pazarçeviren AE, Akbaba S, Evis Z, Tezcaner A. Versatile-in-all-trades: multifunctional boron-doped calcium-deficient hydroxyapatite directs immunomodulation and regeneration. ACS Biomater Sci Eng 2022; 8:3038-53. [PMID: 35708275].

27. Wang S, Yang L, Bai G, Gu Y, Fan Q, Guan X, Yuan J, Liu J. A preliminary study on calcifying nanoparticles in dental plaque: Isolation, characterization, and potential mineralization mechanism. Clin Exp Dent Res 2024; 10:e885[PMID: 38798048].

28. Elshafei AM. SPOTLIGHT ON THE ASSOCIATION BETWEEN NANOBACTERIA AND SOME HUMAN DISEASES Bacterial Empire 2022; 5:e396J.

29. Seymour CO, Palmer M, Becraft ED, Stepanauskas R, Friel AD, Schulz F, Woyke T, Eloe-Fadrosh E, Lai D, Jiao JY, Hua ZS, Liu L, Lian ZH, Li WJ, Chuvochina M, Finley BK,

Koch BJ, Schwartz E, Dijkstra P, Moser DP, Hungate BA, Hedlund BP. Hyperactive nanobacteria with host-dependent traits pervade Omnitrophota. Nat Microbiol 2023; 8:727-44. [PMID: 36928026].

30. Ciorba AL, Teusdea A, Roiu G, Cavalu DS. Particularities of Cataract Surgery in Elderly Patients: Corneal Structure and Endothelial Morphological Changes after Phacoemulsification. Geriatrics (Basel) 2024; 9:77-[PMID: 38920433].

31. Zhu XX, Meng XY, Chen G, Su JB, Fu X, Xu AJ, Liu Y, Hou XH, Qiu HB, Sun QY, Hu JY, Lv ZL, Sun HJ, Jiang HB, Han ZJ, Zhu J, Lu QB. Nesfatin-1 enhances vascular smooth muscle calcification through facilitating BMP-2 osteogenic signaling. Cell Commun Signal 2024; 22:488-[PMID: 39394127].

32. Mu J, Xu F, Guo W, Sun C, Peng B, Huang Q, Fan W. Updated study on demographic and ocular biometric characteristics of cataract patients indicates new trends in cataract surgery. Sci Rep 2025; 15:17289-[PMID: 40389519].

33. Suryani I, Unari U. Posterior Capsule Opacification (PCO) Cases at Lamongan Eye Clinic: Two Years of Retrospective Data. Vision Science and Eye Health Journal 2022; 1:67-71. .

34. Sinani A, Palles D, Bacharis C, Mouzakis D, Kandyla M, Riziotis C. Laser Processing of Intraocular Lenses. Appl Sci (Basel) 2024; 14:6071-.

35. Cabiati M, Vozzi F, Ceccherini E, Guiducci L, Persiani E, Gisone I, Sgalippa A, Cecchettini A, Del Ry S. Exploring Bone Morphogenetic Protein-2 and -4 mRNA Expression and Their Receptor Assessment in a Dynamic *In Vitro* Model of Vascular Calcification. Cells 2024; 13:2091-[PMID: 39768183].

36. Shi Y, Zhang J, Duan W, Gao L, Liu Y. Bone morphogenetic proteins (BMPs) at the forefront of ocular diseases and therapeutics. Eye Vis (Lond) 2025; 12:29-[PMID: 40696418].

37. Datta A, Li XY, Nagpaul M. Early expression of osteopontin glycoprotein on the ocular surface and in tear fluid contributes to ocular surface diseases in type 2 diabetic mice. PLoS One 2024; 19:e0313027[PMID: 39480896].

38. Vipul M. Parmar, Goldis Malek; Investigating the roles of the osteopontin isoforms in retinal pigment epithelium. Invest Ophthalmol Vis Sci 2023; 64:2103-.

39. Nurfahri R, Wahyuni I. NurwasisNurwasis, Djoko Legowo, Ni Putu Ayu Reza Dhiyantari, Made DessyGangga Ayu Cinthiadewi. Expression of bax, Bcl-2, and Bax/Bcl-2 ratio of rattus norvegicus lens epithelial cells as a new approach to compare the protective effects of anti-UV-B glasses and anti-UV-B contact lenses from UV-B radiation: True experimental study in animal models. JournalJournal of Medicinal and Pharmaceutical Chemistry Research. 2024; 11:1237-47. .

40. Maes ME, Donahue RJ, Schlamp CL, Marola OJ, Libby RT, Nickells RW. BAX activation in mouse retinal ganglion cells occurs in two temporally and mechanistically distinct steps. Mol Neurodegener 2023; 18:67-[PMID: 37752598].